Paper presented at Dynamics and Control of Systems and Structures in Space (DCSSS),
6th conference, Riomaggiore, Italy, July 2004

Numerical Simulation of High Velocity Impacts on Thin Metallic Targets II

James Campbell, Rade Vignjevic, Séverine Lepage
Crashworthiness, Impact and Structural Mechanics (CISM)
Cranfield University, UK

Abstract

Spacecraft encounter various impact phenomena in space, among which orbital debris impacts are of most concern. These impacts occur at a wide range of velocities. Impact velocities from a few hundreds m/s to one km/s are common in geostationary orbit and even occur in low Earth orbit. However, these high velocity impacts are not fully characterised. It's required to study the shielding performance in order to assess the spacecraft survivability in the event of high velocity impacts.

The paper is divided into two parts. Overall it investigates the capability of hydrocodes to simulate high velocity impacts. Particular interest is given to the post-penetration debris cloud characterisation and the material failure mode identification. Three different methods were used to simulate the impact of an aluminium sphere on a thin aluminium plate. The first part, considers analyses performed using a finite element model with element erosion and a discrete element method where the problem is modelled with discrete finite elements with nodes tied with breakable linkages. The second part of the paper considers the same problems with the Smoothed Particle Hydrodynamics (SPH) method using the MCM solver developed at Cranfield University.

All three methods showed good agreement in terms of target damage with the available experimental results. However, their performances are different in terms of debris cloud and failure mode characterisation. As a large number of elements are deleted, the element erosion method shows problems in the petaling failure mode representation and doesn't allow the post-penetration debris cloud to be characterised. In order to be more reliable, the SPH method needs improvements, in particular to avoid tensile instability. The discrete element method allows good representation and identification of the failure modes even if some improvements in the definition of the node linkage failure criterion are required.

Introduction

As already mentioned in the first part of the paper the work is intended to support design of protection against low velocity space debris impacts typical for the GEO, orbits characterised by impact velocities range from a few hundreds meters per second to just over one kilometre per second. The same types of impacts occur in LEO on the rear trailing side of spacecraft. For this category of impacts, shock wave based shielding systems are inefficient. The characterisation of the post-penetration fragments is important in order to evaluate the survivability of the spacecraft to these impacts. If the properties of the debris cloud moving inside a

spacecraft are know, it will be possible to develop lethality curves for internal equipment.

Hence, the aim of this study is to investigate the capability of hydrocodes to simulate high velocity impacts. The objectives can be divided into two main tasks:

- The application of modelling methods that can be adequate for the simulation of the phenomena involved in high velocity impacts to representative test cases.
- The comparison of their effectiveness in the determination of the post-penetration fragment characteristics and in the identification of the material failure modes.

In this second part of the paper the SPH method was used to simulate the same impact of an aluminium sphere on an aluminium described in detail in the first part of the paper. Furthermore, a comparison of the results for the three methods the finite element method with element erosion, discrete element method and smooth particle hydrodynamics (SPH) method was performed. Particular attention is paid to the prediction of:

- the hole dimension,
- the target deformation,
- the impact-induced stresses,
- the residual velocity of the projectile,
- the material failure mode,
- the post-penetration debris cloud characteristics.

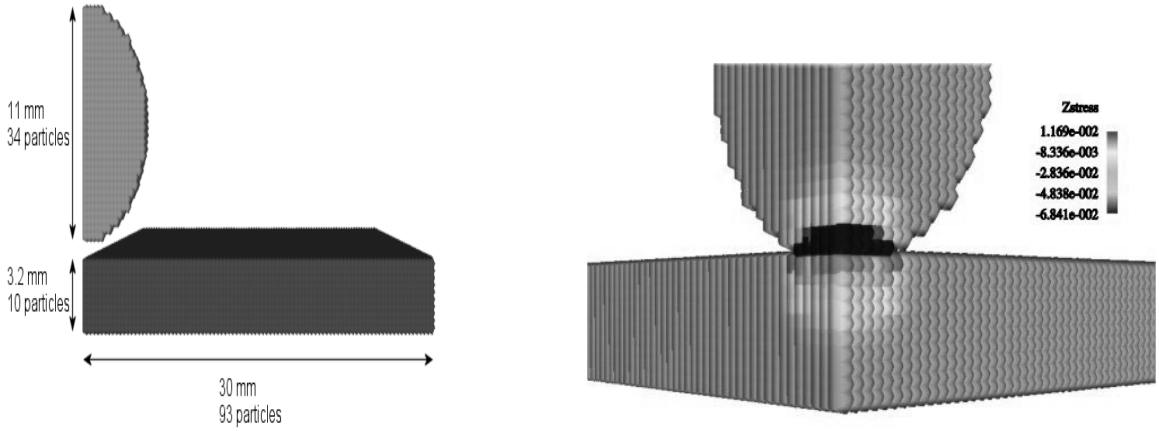
Smooth Particle Hydrodynamics simulations

Smooth Particle Hydrodynamics (SPH) approach is applied to the study of the two test cases. Firstly, the MCM - SPH solver developed at Cranfield University was used. The generation of the SPH model is explained and the results discussed.

MCM, the Cranfield University SPH code, offers some unique features namely a robust ghost particle algorithm for treatment of symmetry planes, silent boundaries and a repulsive force based contact algorithms.

Model generation

Using planes of symmetry only one quarter of the geometry was modelled, (Figure 1). The particles were uniformly spaced in all three Cartesian directions. 34 particles were distributed along the 11-mm diameter of the projectile. In the target, there were 10 particles through the 3.2-mm thickness and 93 along the 30-mm sides. The distance between the boundary particles of the projectile and the target was three times the inter-particle distance so that there was no initial penetration.



(a) (b)

Figure 1: (a) SPH model for the MCM code(b) Z-stress state at time 0.6μs. Unit: 10^2 GPa. (V_{imp} =817 m/s)

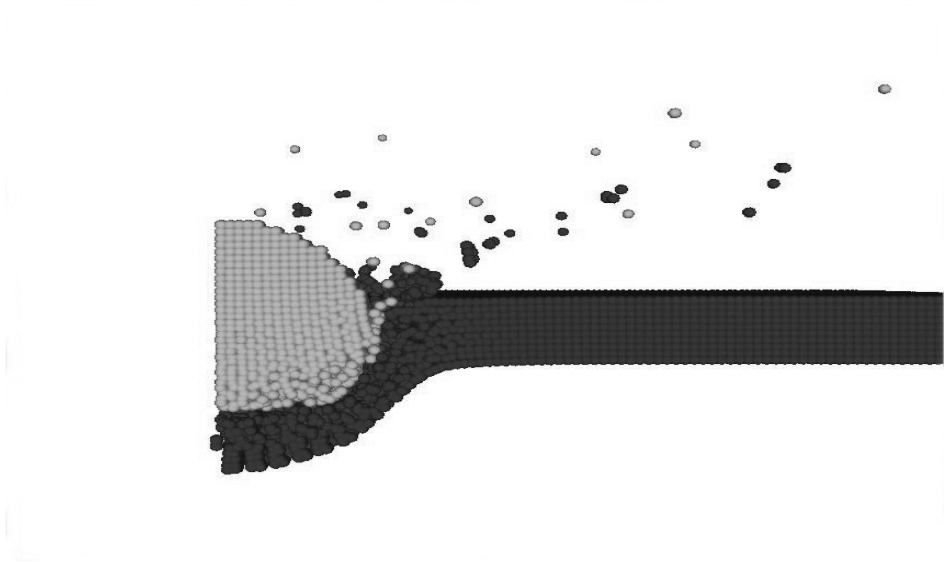


Figure 2: Projectile-target configuration at 15 μs.

For both the projectile and the target, the initial smoothing length was set to 0.4 mm, which was approximately 1.25 times the inter-particle distance. The smoothing length was not constant and varies according to the following relation [1]:

$$h = h_0 \left(\frac{\rho_0}{\rho} \right)^{\frac{1}{3}} \tag{1}$$

An initial velocity of 817 m/s or 500 m/s was applied in the negative z-direction to all the particles of the projectile. The particles on the external plate boundaries were fully constrained.

The contact was modelled using the repulsive force approach. In this, when a boundary particle from a body enters in the sphere of influence of a boundary particle from another body, a repulsive force is applied between these particles [2].

Results

Impact velocity: 817 m/s.

The use of repulsive force contact significantly improved the results. The simulation no more suffers from pronounced zero-energy modes. The contact interface is also clearly defined, no interpenetration occurs between the projectile and the target (Figure 1). However, the clustering of the particles in the back of the plate, shown in Figure 2, illustrates the presence of tensile instability. This has as a consequence the increase of total energy, (Figure 3).

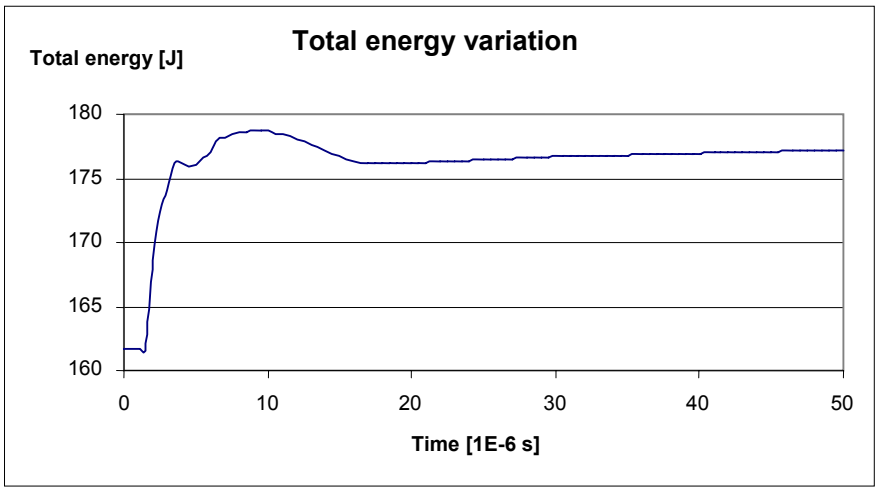


Figure 3: Total energy variation (V_{imp} =817 m/s)

Figure 4 shows the target and projectile after complete perforation. The failure modes that can be identified are plugging and under-developed petaling. Petals are present on the lip of the hole. The post-penetration debris cloud is constituted of several fragments. However, it is difficult to determinate if this fragmentation is due to physical fracture or numerical failure resulting from tensile instability. The plate also experiences dishing. The neutral plane node situated on the edge of the hole (indicated with an arrow in Figure 4) is displaced by 2.8 mm in the negative z-direction at time 50 μs (Figure 5). The plug separates from the projectile after the action of the relief elastic wave while the projectile continues moving at a constant residual velocity, (Figure 5). It should be noted that some particles have lost their neighbours.

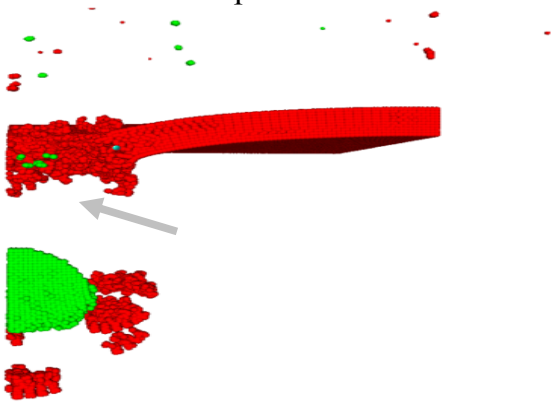


Figure 4: Projectile-target configuration at time 50 μs (V_{imp} =817 m/s). The arrow points to the node whose displacement is plotted in Figure 5

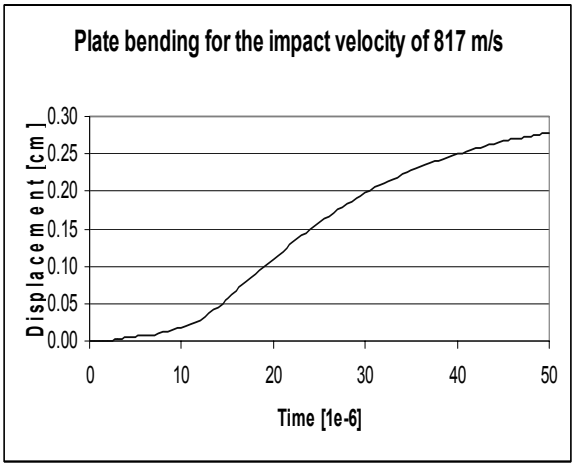


Figure 5: Negative Z displacement of the node marked in Figure 4

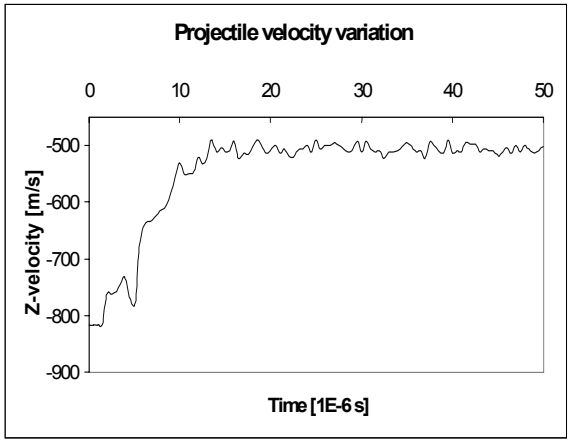


Figure 6: Projectile velocity vs. time (V_{imp} =817 m/s)

The hole radius measured on the top face is 5.98 mm. The height of the projectile is 8.8 mm. The projectile continuously slows down during the first 20 μs until a residual velocity of 500 m/s (Figure 6). The impact-induced z-stress is 8.236 GPa and 5.656 GPa in respectively the projectile and target.

Impact velocity: 500 m/s.

Figure 7 shows that the dominant failure mode is plugging. The plug is not yet separated from the projectile. The hole radius measured on the top face is 5.5 mm. The plate bending can be quantified by the displacement of the node marked in Figure 7. Its maximum displacement is 4.4 mm at 80 μs (Figure 8). The height of the projectile at time 80 μs is 9.2 mm. The projectile slows down from 500 m/s to 275 m/s in 25 μs (Figure 9).

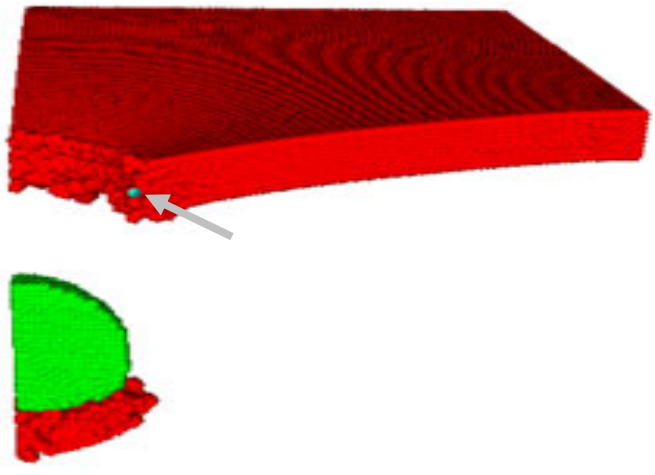


Figure 7: Configuration at time 80 μs (V_{imp} =500 m/s). The arrow points to the node whose displacement is plotted in Figure 8.

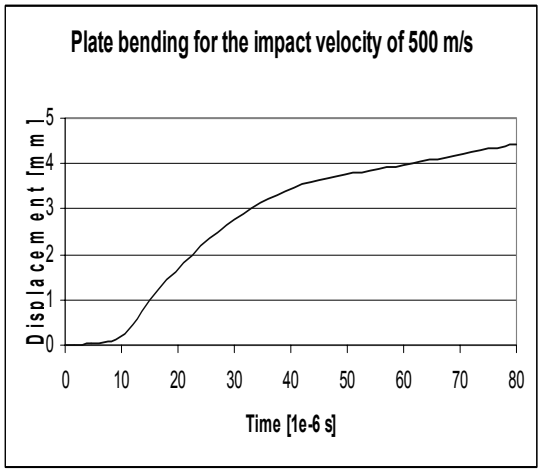


Figure 8: Displacement of the node marked "A" on Figure 6. (V_{imp} =500 m/s)

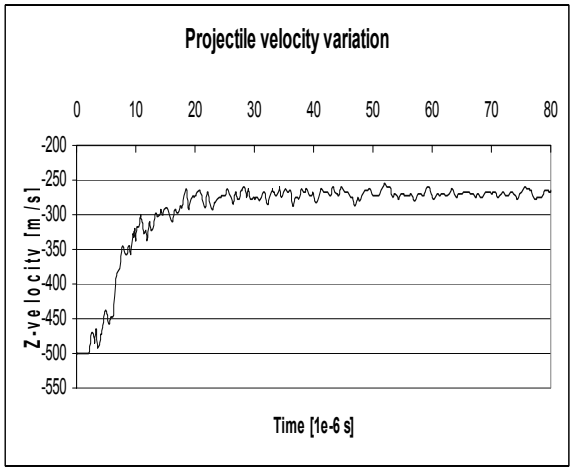


Figure 9: Projectile velocity vs. time

Comparison

Firstly, the quantitative results (e.g. the hole radius, the projectile residual velocity) are compared for the three simulation approaches. Furthermore, their performance in terms of post-penetration debris cloud characterisation and material failure identification is discussed. Finally, their principal drawbacks and merits are discussed.

Quantitative results

Table 1 summarises the results obtained with the different methods for the impact velocity of 817 m/s. The impact-induced stresses are also compared to the 1-D approximation value using Equation 2.

$$\sigma = \rho c v_0 \qquad (2)$$

The wave velocity is assumed to be 5.37 km/s, which is the speed of sound in the unstressed material. The radius of the hole in the target, the residual velocity of the projectile, the impact-induced stress in the projectile and the target, the maximum z-displacement experienced by the target, the final height of the projectile are tabulated.

V_{imp} = 817 m/s	Element Erosion	SPH	Discrete Element	1-D approximation
Hole radius [mm]	5.5	5.9	5.4	N/A
Max z-displacement [mm]	1.64	2.8	2	N/A
Final projectile height [mm]	8.6	8.8	7.7	N/A
Proj. residual velocity [m/s]	607	500	500	N/A
Proj. z-stress at impact [GPa]	5.9	8.2	4.4	6.1
Target z-stress at impact [GPa]	6.6	5.6	4.2	6.1

Table 1: Comparison of numerical results and analytical approximation for impact velocity of 817 m/s

All the values are of the same order of magnitude. The following remarks can be drawn:

- The hole radius is approximately equal to the radius of the projectile. The differences are due to the discretisation of the problem.
- The fact that the projectile is less slowed down in the element erosion simulation might be due to the element deletion in the target so that less resistance is offered to the projectile. This element deletion might also influence the maximum bending deformation of the plate.
- The height of the projectile is more decreased in the discrete element method. This can be explained by the presence of gaps in the model. Indeed, the cumulative height of vacuum introduced along the 11-mm diameter projectile is 1 mm, which corresponds to the difference observed with the other two approach results.
- The impact-induced z-stress is higher in SPH method while discrete element method underestimates it. It should be noted that the variables are stored at successive time intervals and not for every time step. In order to evaluate the impact-induced stress, the storage time interval was set to 0.03 μs to catch the z-stress peak at impact. Hence, care is required when comparing impact-induced z-stress.

In the discrete element method, the artificial gaps introduced between the element influence the results. The deformation of the projectile is more important than for the other two methods. This void also effects the stress. Table 1 compares the available experimental results to the corresponding numerical results. The only available experimental data are the hole radius and the maximum transverse displacement of the plate for the impact velocity of 500 m/s (Bennetti, 2002). The three methods give results in good accordance with the experiments. It should be noted that the dishing deformation of the plate can be influenced by its size. The side dimension was smaller in the simulations than in the experiment. However, the experiments show that the transverse deformation was located near the hole. Therefore, the assumption of an embedded plate of 6-cm side is adequate and gives results comparable.

V_{imp} = 500 m/s	Element erosion	SPH	Discrete element	Experimental results (Bennetti, 2002)
Hole radius [mm]	5.7	5.5	5.7	6
Max z-displacement [mm]	3.1	4.4	3.5	4
Final projectile heigth [mm]	9.4	9.2	8.4	N/A
Proj. residual velocity [m/s]	208	275	180	N/A

Table 2: Comparison of numerical results to available experimental data.
(V_{imp} =500m/s)

To conclude, all three methods give similar quantitative results and are in agreement with the available experimental results.

Failure mode and debris cloud characterisation

The three methods are compared in terms of failure mode and debris cloud characterisation. As spacecraft protection devices are generally constituted of several plates, the debris cloud characterisation after the first perforation is important. Information about this first post-penetration debris is required to study its impact on rear wall. The fragment characteristics are also used to derive lethality curve for the internal equipment to assess the spacecraft survivability if there is no specific shielding system.

For the 500 m/s, all methods predict the perforation by plugging, which is in accordance with the experimental results. However, for the impact velocity of 817 m/s, for which the petaling becomes more important, the methods show different performance.

Element erosion method doesn't provide information on the post-penetration debris cloud. Most of the elements that should constitute the fragments are deleted. The element deletion also makes failure mode identification difficult. Some remains of petals allow the petaling mode identification. However, as no plug is formed and ejected, it's difficult to say if only petaling occurs or if it's a under-developed petaling mode.

The discrete element method improves the debris cloud characterisation and the identification of the failure modes. As shown in Figure 10, the discrete element method (RHS) gives more information on the debris cloud than the element erosion method (LHS). This method allows the under-developed petaling mode to be identified. After the formation of a plug, radial cracks develop creating petals.

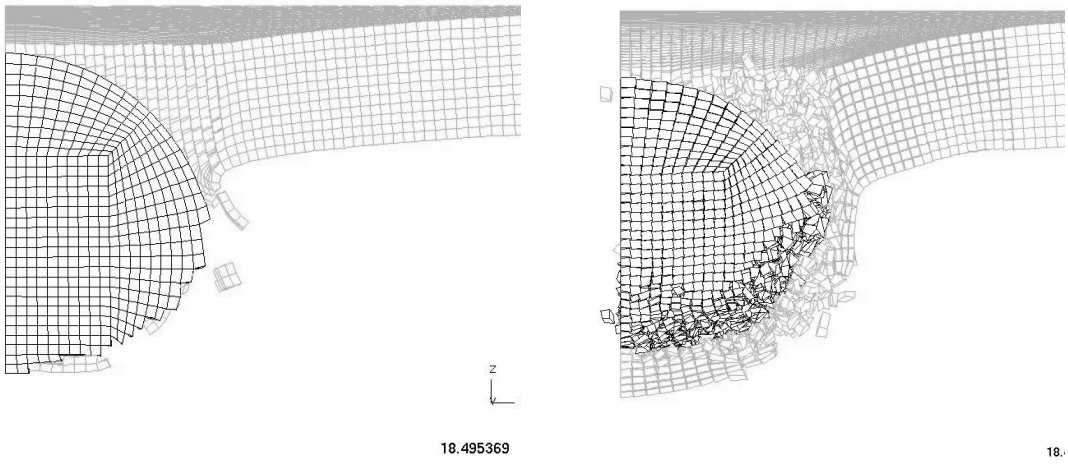


Figure 10: Comparison of the deformation predicted by element erosion method (LHS) and discrete element method (RHS) at time 18.5 µs. (V_{imp} =817m/s)

SPH method produces good representation of the processes even if the post-penetration fragment description might become unreliable because of the tensile instability. Indeed, the plug is divided in several fragments and it's impossible to state if this division is due to physical fracture or to tensile instability.

Method drawbacks and merits

The main drawback of the element erosion method is the physics approximation and loss of information due to the deletion of elements. Another disadvantage is that the simulation results depend on user input. A non-physical element failure strain has to be determined. The reliability of the results depends on the way to tune this value adequately.

The discrete element method also requires the deletion of numerically unstable elements, however fewer elements are deleted than in the element erosion and the deletion occurs when the interaction between the projectile and the target is completed. The main merit is that it allows the identification of the material failure modes. However, it requires some improvements in the failure criterion. The failure forces should be based on flow strength value instead of on quasi-static value. The fitting of these values is not straightforward. A first approach could be to multiply the quasi-static values by a factor but this factor should be determined from corresponding impact tests. The method used to tune the element strain failure is not adequate, as the crater formation doesn't involve the same process as crack propagation. Resnyansky [3] faced the same problem to tune the failure constants even if he used another failure criterion, based on damage accumulation. The code should also be modified to allow strictly coincident nodes to be tied so that artificial gaps will not be required. The fracture is not sharply located. Due to the discretisation, cracks extend over several elements. That generates the separation of single elements, which modifies the debris cloud. This effect might be attenuated by using a radial mesh in the target.

The main advantage of the SPH method over the other two methods is that fewer assumptions are introduced in the modelling process. It doesn't require tuning of parameters such as element failure strain or spotweld failure forces. However, this method can lose reliability because of some problems such as zero-energy modes or tensile instability.

Conclusions

In this work, the capability of hydrocodes in modelling of high velocity impacts has been demonstrated and investigated. High velocity impact test cases were simulated using three different Lagrangian methods:

- Finite element with erosion criterion based on effective plastic strain
- Smooth Particle Hydrodynamics (SPH) method with a repulsive force contact.
- Discrete element method in which the nodes of the discrete elements were tied by breakable spotwelds.

These methods were applied to the simulation of the impact of an 11-mm diameter sphere on a 3.2-mm thick plate. Both the target and the projectile were made of Al2024-T3. Two impact velocities were investigated: 500 m/s and 817 m/s. The simulations provided results in terms of failure mechanisms, hole dimension, residual projectile velocity, projectile and target deformation.

All these methods showed good agreement with the available experimental results, i.e. the hole dimension and maximum transverse displacement of the plate for the

impact velocity of 500 m/s. For the impact velocity of 500 m/s, the dominant failure mechanism is plugging and all methods provide similar results. However, for the impact velocity of 817 m/s, under-developed petaling occurs and the different methods don't show the same performance:

- The element erosion makes the material failure mode identification difficult. Moreover, a significant portion of the post-penetration debris cloud was deleted and removed from the calculations.
- The SPH method suffers of tensile instability that can influence formation of the debris cloud.
- In spite of the fact that the discrete element method introduces assumptions such as failure based on quasi-static failure values and gaps between elements, the results obtained showed its potential in the simulation of material failure mode and debris cloud characterisation.

The main advantages of SPH over the other two methods are it robustness and the independence of the results form user defined constant such as the failure forces.

References

[1] MCM, A 1D/2D/3D Meshless Continuum Mechanic Code for solid and fluid mechanics. User Manual Version 2.0, School of Engineering, Cranfield University, August 2002.

[2] Vignjevic, R., De Vuyst, T., Campbell, J., The use of a homogeneous repulsive force for contact treatment in SPH, *Fifth World Congress on Computational Mechanics*, Vienna, Austria, July 7-12, 2002.

[3] Resnyansky, A. D., DYNA-modelling of the high-velocity impact problems with a split-element algorithm, *International Journal of Impact Engineering*, Vol. 27, Issue 7, pp. 709-727 August, 2002.

Bibliography

[4] Benz, W., Smooth particle hydrodynamics: a review, in J.R. Buchler, editor, *The Numerical Modelling of Nonlinear Stellar Pulsatations*, pp. 269-288, Kluwer Academic Publishers, 1990. Cited in: Campbell, J., Lagrangian hydrocode modelling of hypervelocity impact on spacecraft, PhD thesis, Cranfield University, 1998.

[5] Zukas, J.A., *High velocity impact dynamics*, ISBN 0-471-51444-6, John Wiley & Sons, New York, 1990.

[6] Vignjevic, R., Hughes, K. and Taylor E.A., Finite element modelling of failure of a multi-material target due to high velocity space debris impacts, *Space Debris*, Vol. 2, pp. 41-50, 2002.



https://dspace.org/

Numerical simulation of high velocity impacts on thin metallic targets I and II

Vignjevic, Rade; Campbell, James C.; Lepage, Séverine

2004-12-18T00:00:00Z
http://dspace.lib.cranfield.ac.uk/handle/1826/790

Downloaded from a DSpace repository. https://dspace.org/